Simulating Zebra-Patterned Graphene

Onur Serin

Koç University

25 May 2022

Introduction

- Graphene can used as a passive mode-locker by its saturable absorption property, both in multilayer[2] and monolayer form [3] over a wide wavelength range due to independence of absorption from wavelength
- But insertion loss poses a problem for efficiency, especially for low-gain lasers
- A variety of methods have been proposed to ameliorate the loss such as:
  - Capacitor structures [5][6]
  - Chemical doping [7]
  - **Zebra-patterned graphene** [1]

Capacitor Structures

- Capacitor structures can be designed in a way that when a voltage bias is applied, the Fermi level of graphene is shifted. This affects the optical conductivity of graphene which is proportional to absorption of optical power.
- When the Fermi energy is increased toward half the photon energy for a given frequency, the optical conductivity of graphene approaches half of the value for undoped graphene, resulting in lower absorption [5].
- This effect is viable for lowering insertion loss while allowing enough saturable absorption to achieve mode-locking [5][6]

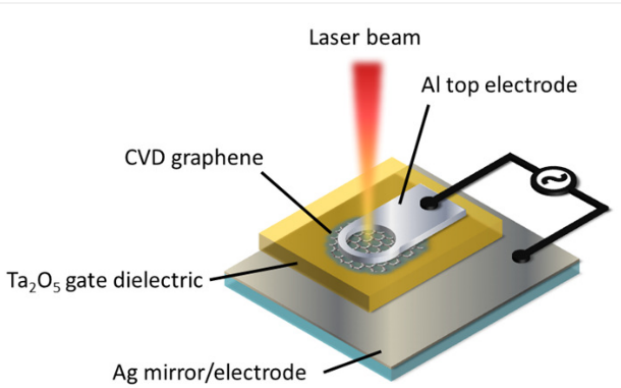

Figure: Capacitor structure from [5]. As for the scale, Ta_2O_5 layer is 225nm thick

Drawbacks

- There are drawbacks to using capacitor structures or chemical doping
  - Capacitor structures introduce reduction in operational wavelength range [6]
  - Chemical doping introduces an irreversible Fermi level shift [7]
- This has pushed researchers to find novel techniques, and in 2020 the Zebra-pattern solution was proposed

Striped Graphene Layers

- The main idea is to have gaps in the graphene layer to decrease the loss but have enough graphene left to still achieve mode-locking.
- By laser micro-manufacturing, one can ablate stripes off a graphene layer. The resulting "zebra-patterns" do not hamper mode-locking when the ratio of unablated area over ablated area is higher than 32% [1].
- The pulse durations decrease with increased ablation ratio as well, which further improves the peak power.

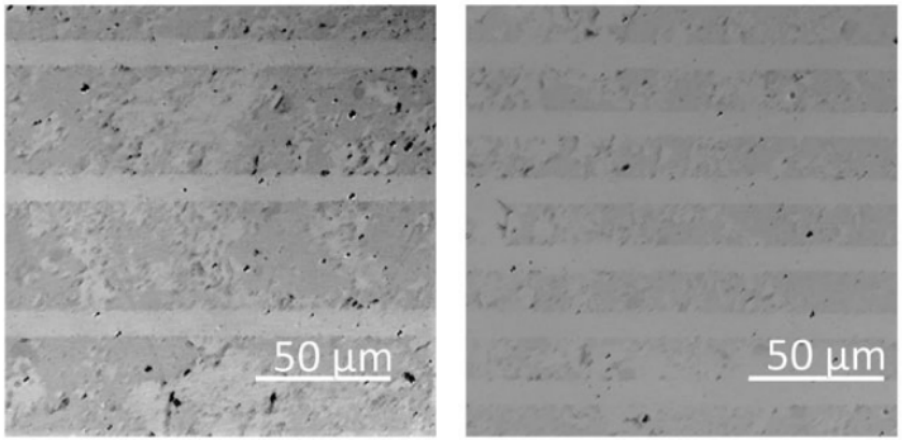

Figure: Confocal microscope images of zebra-patterned monolayer graphene with ablation ratios 19% and 38% respectively[1]

Striped Graphene Layers

Zebra-patterned graphene stripes allow adjusting the loss by changing gap lengths and translation of the graphene layer [1]. This novel technique raises several questions:

- What is the energy loss for an incident laser beam and how does it relate to parameters at hand?
- What is the modulation depth for a striped graphene layer?
- How does relative position and ablation geometry affect energy output?

Simulation

We have composed a simulation toolkit [8] motivated by such questions to investigate how striped saturable absorbant layers affect the fluence of incident beams. With this toolkit, we have been able to devise a formula to predict energy after passage, and calculate loss and modulation depth both by simulation and proposed formulae. We have also investigated how beam ellipticity and the properties of saturable absorber layers affect the efficacy of predictions.

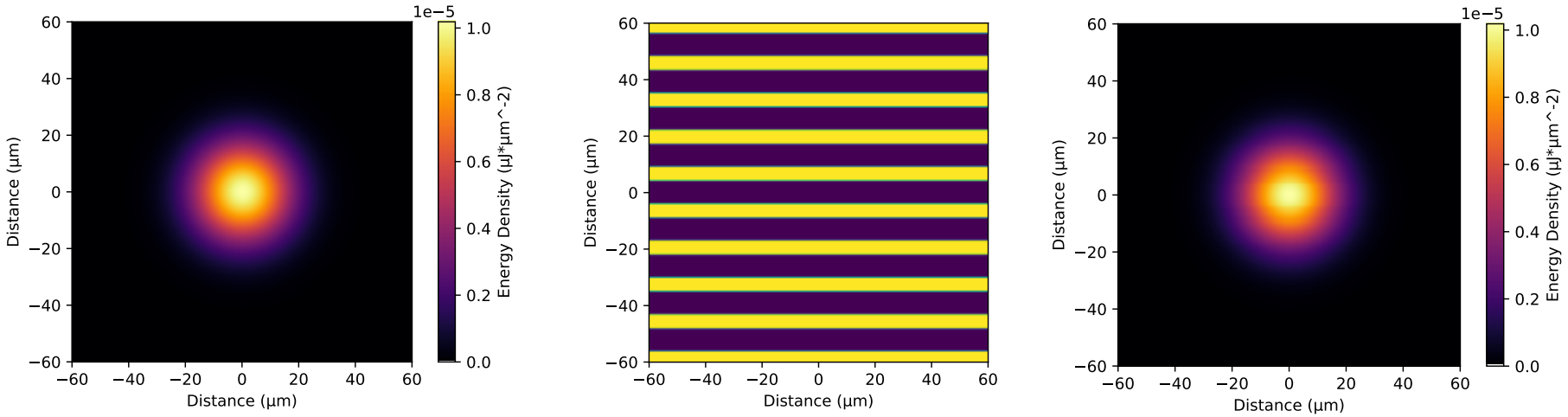

Figure: Energy density plot for an example beam before and after passing through a striped graphene layer as depicted in the middle.

Methodology

In the simulation, a laser beam is represented by a square matrix with entries corresponding to fluence values for points on a plane. Each point is unit length away from the adjacent points. For a Gaussian beam, each entry is calculated by Eq.(1), where $J(x, y)$ stands for fluence at (x, y), E_p for the total energy on the plane and w for the radius of the beam waist. As for ellipticized variants of Gaussian beams tilted at an angle θ, we use Eq.(1a).Angle θ represents the horizontal tilt of the plane of the graphene layer.

$$J(x, y) := \frac{2E_p}{\pi w^2} e^{\frac{-2}{w^2}(x^2+y^2)} \tag{1}$$

$$J(x, y) := \frac{2E_p \cos(\theta)}{\pi w^2} e^{\frac{-2}{w^2}(x^2 \cos^2(\theta)+y^2)} \tag{1a}$$

Methodology

The center of the matrix holds the value for J(0,0). The chosen dimensions of a beam matrix should ensure that the discretized calculation of E_p by Eq.(2) yields a close enough value to actual E_p, which is the result of integrating J(x,y) of Eq.(1) over the whole plane.

$$E_p \approx \sum_{\text{plane}} J(x, y) \cdot A, \text{ where } A := (\text{unit length})^2 \tag{2}$$

A graphene layer is represented by a matrix with entries of 1s and 0s, which stand for presence of graphene at the corresponding location or lack thereof, respectively. The dimensions of a graphene layer matrix is tailored for matching an already initialized laser beam. A layer also has the following associated constants pertaining absorption: α_0 for the linear absorption rate, α_s for the saturable absorption rate, and J_s for the saturation fluence.

Methodology

A passage of a beam through a layer results in a new beam matrix, by which the new E_p value of the resultant beam can be calculated using Eq.(2). Each J value in the matrix of the passing beam is subject to either of the following operations: It is copied to the new beam matrix with the same index, if the corresponding entry on the layer matrix with the same index is 0. Otherwise, Eq.(3) is used to yield the new J value. $\Delta J(J)$ is the loss in fluence function.

$$J_{new} = J - \Delta J(J), \text{ where } \Delta J(J) := J \cdot (\alpha_0 + \frac{\alpha_s}{1 + J/J_s}) \tag{3}$$

Graphene layers of interest for us are the ones with a repetitive pattern of stripes of graphene and gaps in between. The width of the graphene stripes and gaps are fixed, represented by d_{gph} and d_{gap} respectively, whereas d_{tot} will stand for $d_{gph} + d_{gap}$ which is the width of one period.

Energy

Moving on to proposing of formulae, let us define the parameter R as the ratio $\frac{d_{gph}}{d_{tot}}$. We can approximate the planar energy after passage by a "miniscule stripes approximation" as in Eq.(4).

$$E_{msa} \approx E_p - R \iint_{-\infty}^{\infty} \Delta J dx dy \tag{4}$$

There is no significant variation depending on the relative position of the graphene layer for $d_{tot} < w$ and Eq.(4) holds regardless of translation in space. This holds for Gaussian beams, as well as their tilted, ellipticized variants that have their major axes parallel to the stripes. As for $d_{tot} > w$, there is considerable variation depending on the position of the graphene layer

Translation

For $d_{tot} > w$, we introduce the following formula:

$$E_{after} \approx E_{msa} \cdot \left[1 + c\frac{d_{tot} - w}{w} \cdot \sin(2\pi\frac{y}{d_{tot}})\right] \tag{5}$$

The variable y in Eq.(5) corresponds to the relative position. When $y = d_{tot}/4$, the center of the beam hits the center of a graphene stripe, resulting in maximum loss. When $y = 3d_{tot}/4$, the center of the beam hits the center of a gapped stripe, resulting in minimum loss. The variation over one period is hypothesized to be sinusoidal and $E_{msa} \cdot c\frac{d_{tot}-w}{w}$ is the variation amplitude, where c is a constant. When the constant c is calibrated for $R \approx 0.5$, it yields accurate results compared to simulations of practical application cases covered by Morova et al. [1]

Translation - Clipping

- However, in Eq.(5), there is the problem of not being bounded above as d_{tot} increases when the rest of the parameters stay constant. The variation introduced by translation must converge to a finite value, with the maximum energy value (which is the E_p of the incident beam) corresponding to supposing an all-empty layer and the minimum energy value (E_{min}) calculable by Eq.(4) by supposing a graphene layer with no gaps, i.e. $R = 1$.
- On top of Eq.(5), we can introduce a clipping condition to overcome this defect as follows: E_{after} values below E_{min} are reassigned as E_{min} and values above incident E_p are reassigned as E_{max}. This suffices for a good fit to simulations for $d_{tot} \gg w$.

Modulation Depth

Modulation depth can be defined as the percent change from the mean loss to max/min loss for a fixed position of the graphene layer, with E_p, the total energy on the plane being the free variable to alter to get maximum/minimum loss and the rest of the parameters stay constant. We can heuristically argue that the modulation depth M is:

$$M \approx \frac{100}{2} \frac{\alpha_s}{\alpha_s + \alpha_0} \ \% \tag{6}$$

Modulation Depth

We can proceed as follows: Let E_p^h, E_p^l denote a "very high" and "very low" total energy of the plane for a beam, which will result in minimum and maximum loss respectively by (3). By the approximation of Eq.(4) and taking fluence J on the whole plane to infinity and zero for E_p^h, E_p^l respectively, we get:

$$E_{msa}^h \approx E_p^h - R\alpha_0 E_p^h$$

$$E_{msa}^l \approx E_p^l - R(\alpha_0 + \alpha_s) E_p^l$$

Now, note that we fix an arbitrary position for the graphene layer, and the square bracketed part of (5) is the same for both E_p^h and E_p^l, let us call it β. Thus $E_{after}^h \approx \beta E_{msa}^h$ and $E_{after}^l \approx \beta E_{msa}^l$. The loss ratio for any given configuration is $L := 1 - \frac{E_p - E_{after}}{E_p}$.

Then $L^h = \beta R\alpha_0$ and $L^l = \beta R(\alpha_0 + \alpha_s)$. Finally,

$M = 100 \frac{\text{max L - mean L}}{\text{max L}} \approx 100 \frac{L^l - L^h}{2} / L^l = \frac{100}{2} \frac{\alpha_s}{\alpha_s + \alpha_0}$.

Data

By using the simulation code and the previous formulae, we can calculate values of interest such as loss, energy over a translative period, and modulation depth. We will look into data collected for monolayer graphene, whose parameters are taken as

- $\alpha_0 = 1.61 \times 10^{-2}$, $J_s = 1.45 \times 10^{1}$ uJcm^{-2}
- Total absorption loss ratio $= 2.3 \times 10^{-2}$ [4]
- And we can take $\alpha_s = 2.3 \times 10^{-2} - 1.61 \times 10^{-2} = 6.9 \times 10^{-3}$.
- For these parameters, Eq.(5) was calibrated by $c = 2 \times 10^{-3}$.

In the experimental setup of [1], graphene layers had a fixed ablation thickness of 9.3um, and Gaussian beams were incident to the plate at the Brewster angle for a refractive index of 1.45 for the material, with $w = 34$um and $E_p = 3 \times 10^{-4}$uJ. We multiply loss by 2 to account for two passes. In the figure below, we can observe that translation causes a sinusoidal-like change in energy after passage as hypothesized by Eq.(5), and that the position dependence of the graphene layers become negligible for $R > 30\%$, which is concordant with the hypothesis that $d_{tot} < w$ results in negligible translational variance as $d_{tot} \leq 31 < w = 34$um for $R > 30\%$.

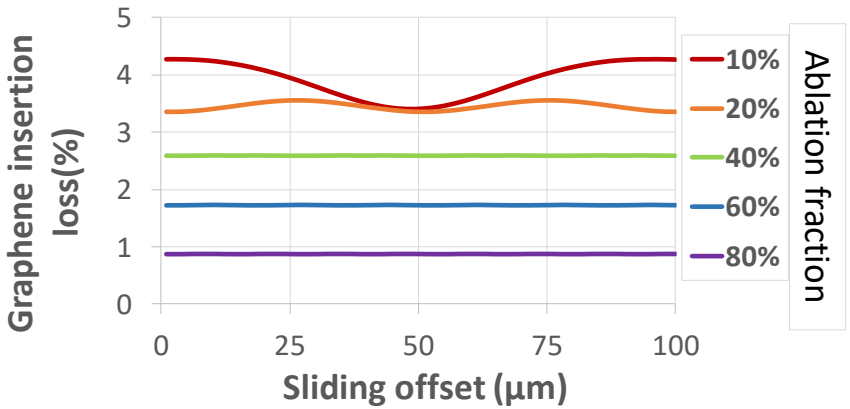

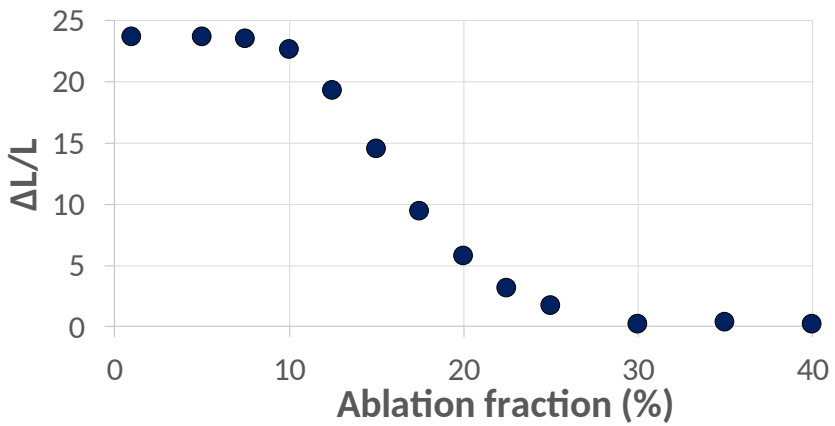

Figure: Left: Calculated variation of loss as the beam is translated over a monolayer graphene for different ablation fractions. Right: Calculated variation of the maximum fractional loss change as a function of ablation fraction. Published in [9]

E_p	w	d_{tot}	$\%_{gph}$	@max	@min
$1.0 \cdot 10^{-1}$	20	40	0.3	0.019	-0.050
$1.0 \cdot 10^{-1}$	20	40	0.7	0.012	-0.062
$1.0 \cdot 10^{-3}$	20	40	0.3	0.026	-0.051
$1.0 \cdot 10^{-3}$	20	40	0.7	0.026	-0.056
$1.0 \cdot 10^{-3}$	20	50	0.3	0.061	-0.12
$1.0 \cdot 10^{-3}$	20	50	0.7	0.091	-0.092
$1.0 \cdot 10^{-3}$	30	40	0.3	-0.020	0.020
$1.0 \cdot 10^{-3}$	30	40	0.7	-0.018	0.020
$1.0 \cdot 10^{-3}$	30	50	0.3	0.0059	-0.0076
$1.0 \cdot 10^{-3}$	30	50	0.7	0.0097	-0.0070
$1.0 \cdot 10^{-5}$	20	40	0.3	0.11	-0.15
$1.0 \cdot 10^{-5}$	20	40	0.7	0.11	-0.16
$1.0 \cdot 10^{-5}$	20	50	0.3	0.18	-0.27
$1.0 \cdot 10^{-5}$	20	50	0.7	0.22	-0.24
$1.0 \cdot 10^{-5}$	30	40	0.3	0.011	0.0011
$1.0 \cdot 10^{-5}$	30	40	0.7	0.021	0.0092
$1.0 \cdot 10^{-5}$	30	50	0.3	0.069	-0.058
$1.0 \cdot 10^{-5}$	30	50	0.7	0.081	-0.051

Figure: Percent error table for Eq.(5) with respect to the resultant E_p values of Gaussian beams in simulation, max and min refer to the maxima and minima for one translative period. Units are uJ, um. Minus sign indicates overestimation, lack thereof indicates underestimation.

Data

- The percent error table compares the maxima and minima of the output of Eq.(5) with simulations over a translative period for various example parameters for Gaussian beams.
- We have also calculated percent errors for the ellipticized variants of Gaussian beams tilted at the Brewster angle of infrasil, for the same parameters in the table. When the major axis is parallel to the stripes, the results are promisingly similar. However, for ellipticized Gaussian beams whose major axes are not parallel to the stripes, Eq.(5) needs further adjustment to yield low error results. For the case of major axis being perpendicular to the stripes, swapping w with $w \cdot \tan(\theta_{tilt})$ in Eq.(5) yields low percent errors comparable to the parallel case.

Data

Calculations of modulation depth using the configurations in the table with monolayer graphene parameters through scanning in the energy range 10^{-10} uJ $\leq E_p \leq 10^{11}$ uJ concur up to 4 significant figures with the prediction of (6) which asserts that $M \approx 15\%$. This points out that M is independent of w, d_{tot}, R as expected.

Data

- The constant c of Eq.(5) depends on the α_0, α_s and J_{sat} parameters of the saturable absorber layer.
- As well as affecting c, there is a peculiarity introduced by high α_0 and α_s values. While keeping other parameters the same, increasing α_0 or α_s linearly decreases the average resultant E_p, and this decrease is stronger for α_0.
- This means that using Eq.(4),(5) will result in more error as α_0 or α_s is taken higher and higher, and there seems to be no simple way of estimating the shift precisely for a given set of parameters.
- However, this is not a serious issue as the effect is minimal for practical cases dealing with graphene. Even at a very high non-saturable loss of $\alpha_0 = 0.15$, the shift of the average with respect to the estimated one by Eq.(5) is on the order of 0.1% while keeping α_0 small, and a very high saturable loss of $\alpha_0 = 0.15$ introduces an even smaller shift while keeping α_s small.

Data

Note that the constant c can be calibrated for saturable absorber layers other than monolayer graphene. For example, we can use the following constants for double-layer graphene:

- $\alpha_0 = 3.05 \times 10^{-2}$, $J_s = 2.25 \times 10^{1}$ uJcm^{-2},
- Total absorption loss ratio $= 4.6 \times 10^{-2}$ [4]
- And we can take $\alpha_s = 0.046 - 0.0305 = 1.55 \times 10^{-2}$

The percent error values in the table has also been calculated for the same parameters for the double-layer graphene case by calibrating the constant c to $c = 4 \times 10^{-3}$, which yields similar error percentages compared to monolayer graphene.

Discussion

In this work, only stripes have been considered due to their ease of manufacturing, but other geometries such as circular patterns could be investigated as well, and this can be readily done by extending the layer initialization part of the code.

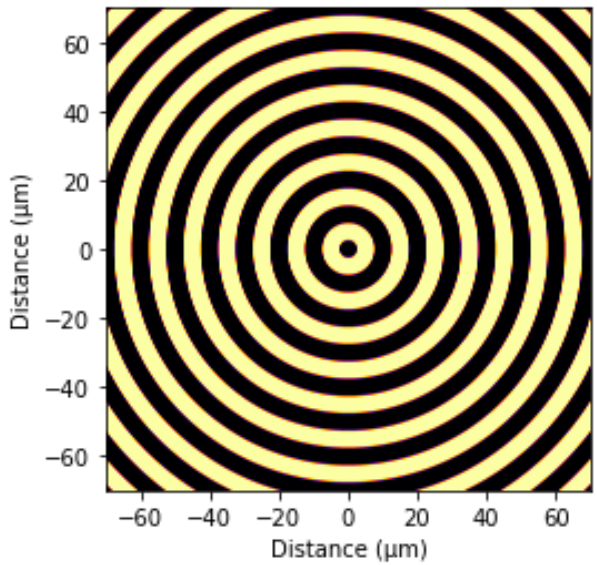

Figure: Representation of a graphene layer with circular ablations 5um thick with 5um thick graphene stripes in between

Discussion

- Morova et al.[1] has found that zebra-patterned graphene layers make pulsees shorter in duration compared to unablated graphene, see figure below
- This motivates us to investigate the beam pulse durations. The durations might be correlated to the effective J_{sat} value of a zebra-patterned graphene, which we define as the J_{sat} value corresponding to an unablated graphene layer which would yield the same loss due to saturable absorption for a given beam compared to the zebra-patterned one.

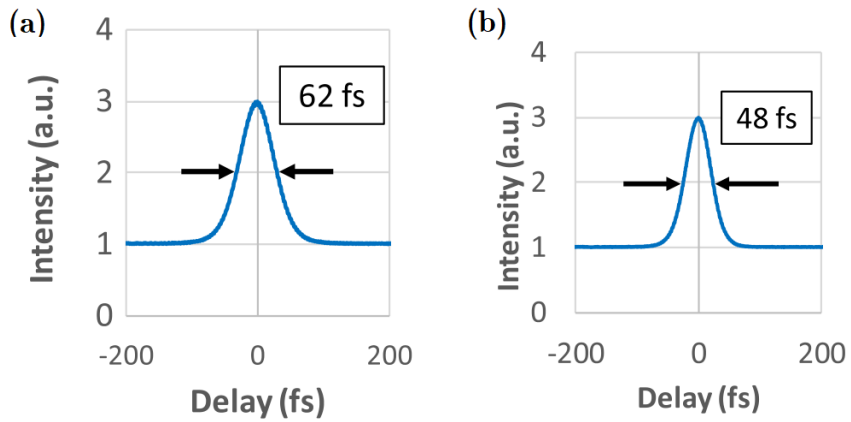

Figure: Intensity autocorrelation trace for unablated graphene (a) and zebra-patterned graphene (b) [1]

[1] Y. Morova, J.E. Bae, F. Rotermund, and A. Sennaroglu, "Laser-micromachined zebra-patterned graphene as a mode locker with adjustable loss," Optics Letters **45**, 1826–1829 (2020).

[2] H. Zhang, D.Y. Tang, L.M. Zhao, Q.L. Bao, and K.P. Loh, "Large energy mode locking of an erbium-doped fiber laser with atomic layer graphene," Optics Express **17**, 17630–17635 (2009).

[3] C.C. Lee, G. Acosta, J.S. Bunch, and T.R. Schibli, "Mode-locking of an Er:Yb:glass laser with single layer graphene," International Conference on Ultrafast Phenomena, TuE29 (2010).

[4] W.B. Cho, J.W. Kim, H.W. Lee, S. Bae, B.H. Hong, S.Y. Choi, I.H. Baek, K. Kim, D. Yeom, and F. Rotermund, "High-quality, large-area monolayer graphene for efficient bulk laser mode-locking near 1.25um," Optics Letters **36**, 4089–4091 (2011).

[5] C.C. Lee, S. Suzuki, W. Xie, and T.R. Schibli, "Broadband graphene electro-optic modulators with sub-wavelength thickness," Optics Express **20**, 5264–5269 (2012).

[6] I. Baylam, M.N. Cizmeciyan, S. Ozharar, E.O. Polat, C. Kocabas, and A. Sennaroglu, "Femtosecond pulse generation with voltage-controlled graphene saturable absorber," Optics Letters **45**, 5180–5183 (2014).

[7] H. Liu, Y. Liu, and D. Zhu, "Chemical doping of graphene," Journal of Materials Chemistry **21**, 3335–3345 (2011).

[8] O. Serin, "Simulation Toolkit for Laser Beams Masked by Semi-ablated Saturable Absorbant Surfaces," (2020) https://github.com/serinos/beam-graphene/

[9] Y. Morova, O. Serin, J.E. Bae, F. Rotermund, and A. Sennaroglu, "Femtosecond Pulse Generation Using Laser Written Zebra Patterned Graphene with Adjustable Loss," Laser Congress 2020 (ASSL, LAC), Paper JTh2A.28 (2020).